Domain Organization and a Protease-Sensitive Loop in Eukaryotic Ornithine Decarboxylase†

Andrei L. Osterman, Deirdre V. Lueder, Mary Quick, David Myers, Bertram J. Canagarajah, and Margaret A. Phillips*

Department of Pharmacology, University of Texas Southwestern Medical Center, Dallas, Texas 75235

Received June 7, 1995; Revised Manuscript Received August 8, 1995⊗

ABSTRACT: *Trypanosoma brucei* ornithine decarboxylase was reconstituted by coexpression of two polypeptides corresponding to residues 1−305 and residues 306−425 in *Escherichia coli.* The two peptides were coexpressed, at wild-type levels, from a single transcriptional unit that was separated by a 15-nucleotide untranslated region containing a ribosome binding site. The fragmented enzyme was purified and analyzed. The N- and C-terminal peptides are tightly associated into a fully active tetramer which has the same molecular weight as the native dimer. The kinetic constants (K_m and k_{cat}) measured for the decarboxylation of ornithine are identical to those obtained for the wild-type enzyme. These results suggest that the enzyme is organized into two structural domains, with a domain boundary in the region of amino acid 305. In contrast, the individual N- and C-terminal peptides are expressed primarily as inclusion bodies. Small quantities of soluble N-terminal peptide could be purified. This truncated protein is capable of inhibiting the wild-type enzyme, suggesting that it is folded into a native-like structure. Limited proteolysis with trypsin or chymotrypsin identifies a likely surface loop at amino acids 160−170, present in both the mouse and *T. brucei* enzyme, which positions one or more functionally important active site residues (e.g., Lys169). Kinetic analysis of a chimeric enzyme composed of *T. brucei* and mouse ornithine decarboxylase suggests that the substrate carboxylate binding determinant is located between residues 1 and 170.

Ornithine decarboxylase (ODC)[1] catalyzes the first step in polyamine biosynthesis, the decarboxylation of ornithine to produce putrescine. Because polyamines are required for cell growth and differentiation (Tabor & Tabor, 1984), inhibitors of ODC have been tested as antiparasitic and antitumor agents (Marton & Pegg, 1995). A suicide inhibitor of ODC, α-difluoromethylornithine, cures *Trypanosoma brucei* infection in man (Wang, 1995). Further progress toward the design of additional therapeutic ODC inhibitors requires a better understanding of the structural organization of the enzyme.

Eukaryotic ODC is a pyridoxal-5′-phosphate (PLP) dependent enzyme, functioning as a homodimer with two equivalent active sites that are formed at the dimer interface (Tobias & Kahana, 1993). The eukaryotic ODCs are related to bacterial and plant arginine decarboxylases and bacterial diaminopimelate decarboxylases (Grishin et al., 1995). They are unrelated to bacterial ODC, for which the structure has been recently solved (Momany et al., 1995). Despite the lack of crystallographic data, some important structural elements have been localized to the active site of eukaryotic ODC: Lys69 forms a Schiff base with PLP (Coleman et al., 1993; Poulin et al., 1992), Glu274 interacts with the pyridine nitrogen of PLP (Osterman et al., 1995), and Cys360 is labeled by α-difluoromethylornithine (Poulin et al., 1992). The conclusion that ODC has shared active sites was based on the observation that activity is restored upon mixing of the inactive K69A and C360A mutant enzymes (Tobias & Kahana, 1993). Finally, site-directed mutagenesis has identified a number of other residues which are required for full enzyme activity (Lu et al., 1991; Tsirka & Coffino, 1992; Coleman et al., 1994; Osterman et al., 1995).

The domain organization of ODC has not been experimentally detailed. Several lines of evidence indicate that ODC is composed of at least two structural domains, a N-terminal domain of approximately the first 300 amino acids and a smaller C-terminal domain containing the remaining residues. First, multiple amino acid sequence alignment of the eukaryotic ODCs and related bacterial decarboxylases reveals that the junction region between amino acid 300 and 340 varies in length from 40 amino acids in mouse ODC to 115 amino acids in *Escherichia coli* arginine decarboxylase (Grishin et al., 1995). This is the only region within the sequence alignment where long insertions are observed. Second, mutations in ODC fall into two groups segregated by their position in the amino acid sequence. Catalytic activity is partially restored only in heterodimers formed upon the mixing of group one ODC mutants (residues 69−274) with group two (residues 360−

† This work was supported by grants to M.A.P. from the Welch foundation (I-1257) and the National Institute of Health (R01 AI34432-01A2).

* Corresponding author. Phone: 214-648-3637. Fax: 214-648-2971. E-mail: Philli01@UTSW.swmed.edu.

⊗ Abstract published in *Advance ACS Abstracts,* September 15, 1995.

[1] Abbreviations: ODC, ornithine decarboxylase; tbODC, *Trypanosoma brucei* ODC; mODC, mouse ODC; PLP, pyridoxal-5′-phosphate; DTT, dithiothreitol; mutant ODCs are referred to by their single-letter amino acid code, e.g., K69A for the Lys69 to Ala mutant. Mouse ODC numbering is used as the standard. The protein fragments of ODC and their expression constructs are abbreviated by the amino acid position used for fragmentation, where N is the N-terminal peptide starting at amino acid 1 going to the defined position and C is the C-terminal peptide which begins at the defined position and continues to the protein stop site. T is for fragments from tbODC, and M is for mODC. For coexpression of two fragments, the start site of the C-terminal peptide is indicated, e.g., TΔ306C.N corresponds to the coexpression product of tbODC peptides 1−305 and 306−425; Δ indicates that the His-tag was deleted from the C-terminal peptide.

0006-2960/95/0434-13431$09.00/0

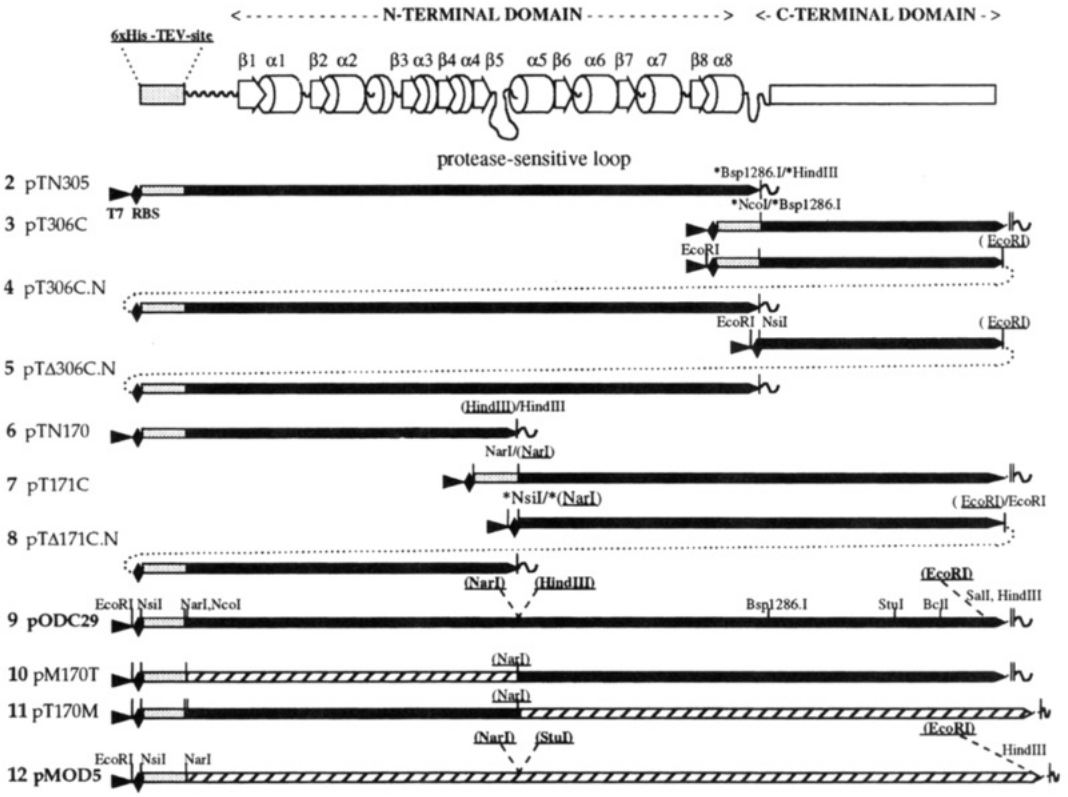

FIGURE 1: Major plasmid constructs for expression of tbODC peptide fragments: 2−5, putative domains; 6−8, proteolytic fragments; and 10, 11 chimeras between tbODC-9 and mODC-12. The constructs numbers correspond to the lane numbers in Figure 2. The position of the T7 promoter is shown with an arrow and the ribosome-binding sequence with a diamond. Coding sequence segments of tbODC are black, those of mODC are hatched, and those of tag-peptide regions are shadowed. Only relevant restriction sites are shown, sites modified by cloning are marked with an asterisk, and engineered restriction sites are shown in parentheses and underlined. A diagram of the ODC structural organization, shown in the upper row, is based on the predicted secondary structure (Grishin et al., 1995): arrows represent predicted β-strand elements, cylinders represent predicted α-helices, and wavy lines represent predicted loops. The His_6tag-peptide and the C-terminal domain are shown as rectangles.

364) ODC mutants (Coleman et al., 1994; Osterman et al., 1995). Finally, sequence analysis provides evidence that ODC may be related to alanine racemase (Grishin et al., 1995). Alanine racemase is composed of two domains with the domain boundary occurring in the region corresponding to amino acid 300 in ODC (Galakatos & Walsh, 1987; Toyama et al., 1991).

In the absence of crystallographic data, several functional tests have been used to delineate the domain organization of a protein, including limited proteolysis and the reconstitution of active enzyme from coexpressed fragments corresponding to the putative domains [e.g., alanine racemase (Galakatos & Walsh, 1987; Toyama et al., 1991) and aspartate transcarbamoylase (Powers et al., 1993; Yang & Schachman, 1993)]. We applied these approaches to characterize *T. brucei* ODC. Coexpression of two polypeptides corresponding to residues 1−305 and residues 306−425 produced soluble active enzyme, suggesting that ODC consists of a large N-terminal domain and a smaller C-terminal domain. Limited proteolysis of *T. brucei* and mouse ODC suggests that amino acids around 160−170 form part of a protease-sensitive loop which plays an important role in the structural organization of the active site.

EXPERIMENTAL PROCEDURES

Materials

The CO_2-detection kit, trypsin, and chymotrypsin were purchased from Sigma; Ni^{2+}-NTA agarose was purchased from Qiagen. Agarose with immobilized soybean trypsin inhibitor was a product of Pierce.

Methods

Mutagenesis. Site-directed mutagenesis was performed as described (Kunkel, 1985) in the Bluescript KS- (Stratagene) vector using helper phage R408 (Stratagene) and *E. coli* strain BO265. Altered nucleotides are shown in lower case, and amino acid substitutions are shown in parentheses (see below). Minimal fragments containing mutations were transferred to the corresponding expression constructs and verified by DNA sequencing.

Expression Constructs. Plasmids pODC29 and pMOD5 (Osterman et al., 1994), containing the full-size genes of *T. brucei* and mouse ODC fused at the N-terminus to the codons for six histidines (His_6-tag) and the TEV protease site, were used to construct all other plasmids which are described below and in Figure 1.

Plasmid pTN305. pODC29 was digested with Bsp1286I, treated with T4-polymerase to produce blunt ends, and further digested with *Eco*RI. The 1 kb fragment containing residues 1−305 was ligated into the 2.2 kb vector derived from pODC29 by digestion with *Hin*dIII, T4-polymerase treatment, and *Eco*RI digestion. The 5′-end of the N-terminal peptide expressed from this plasmid is identical to pODC29, the 3′-end is A305-YR-stop codon (TGA).

Plasmid pT306C. The 0.4 kb Bsp1286I fragment of pODC29, blunted with T4-polymerase, was digested with

*Bcl*I. The 0.25 kb fragment was ligated to a 2.9 kb fragment derived from pODC29 by digestion with *Nco*I, T4-polymerase treatment, and *Bcl*I digestion. The 5′-end of the C-terminal peptide expressed from this plasmid contains one extra Met residue between the original H_6-TEV tag-sequence and the ODC sequence starting at H-306. The 3′-end is identical to pODC29.

Plasmid pT306C.N. The 0.8 kb *Stu*I−*Sal*I fragment of pODC29, modified to insert an *Eco*R1 site by site-directed mutagenesis at the 3′-end of the ODC gene, was ligated with the *Stu*I−*Sal*I 2.2 kb fragment of pT306C. The oligonucleotide used for the mutagenesis was GTTGAAAAG-TCtAgAATtcTAAATGGAAGCG (QKS422-425- > LEF). The 430 bp *Eco*RI fragment from this construct, containing the ribosome binding site (RBS) and the whole C-terminal domain coding sequence, was cloned into the *Eco*RI site of pTN305. The generated cotranslational unit consists of the 5′-region of pT306C modified so that the three terminal amino acids are LEF instead of QKS followed by the TAA-stop codon. The latter immediately precedes the second RBS (GGAGG) of the N-terminal peptide translational unit of pTN305. The intercistronic region of the construct is

```
                    EcoRI
..............  gAA Ttc TAA GGAGGTTTAACC ATG ..............
C-terminal peptide. Glu Phe stop            Met.N-terminal peptide
                    425                     -16
```

Plasmid pTΔ306C.N. This plasmid is identical to pT306C.N except that the 48 base pair *Nsi*I fragment containing the His_6-tag sequence was deleted from the 5′-end of the C-terminal peptide.

Other Constructs. Plasmid pTN170, pT171C, pTΔ171C.N, pT170M, and pM170T were created using similar methods. The introduced restriction sites used in their construction are displayed in Figure 1. Complete details are available upon request.

Expression and Purification of ODC. Small-Scale Expression of Multiple Constructs. Fifty milliliter cell cultures of *E. coli* B21/DG3 containing the construct of interest were induced for protein expression as described (Osterman et al., 1994). Cells were lysed by sonication in A_h buffer (25 mM HEPES-NaOH, pH 7.0, 100 mM NaCl, 5 mM β-mercaptoethanol, 0.015% Brij-35, and 20 μM PLP) plus 2 mM PMSF, and the soluble fractions were loaded onto 150 μL Ni^{2+}-NTA agarose minicolumns. Columns were washed in A_t buffer (50 mM Tris-HCl, pH 8.0, is substituted for HEPES in A_h buffer), A_t buffer plus 1 M NaCl, A_h buffer, and A_h buffer containing 40 mM imidazole. Bound protein was eluted with A_h buffer containing 200 mM imidazole. The cell pellets were resuspended in A_t buffer containing 7 M urea before processing on the Ni^{2+}-NTA agarose minicolumns. All further steps are the same as for the soluble fractions, but 6 M urea is included in all buffers and the 40 mM imidazole wash is skipped.

Large-Scale Expression and Purification of Selected Constructs. Protein was expressed and purified from *E. coli* B21/DG3 cultures containing the construct of interest by purification on Ni^{2+}-NTA agarose and Hi-Load 16/60 Superdex 200 (Pharmacia) gel-filtration as described (Osterman et al., 1994).

ODC Activity Assay and Kinetic Analysis. Decarboxylation of L-ornithine was followed by a coupled spectral assay using the CO_2-detection kit as described (Osterman et al., 1994). For routine assays 10 mM ornithine was used; for K_m and k_{cat} determination, the ornithine concentration ranged from 0.05 to 5 mM. The program "k_{cat}" (Biometallics, Inc.) was used for calculations.

For urea inactivation studies ODC samples (0.25 mg/mL) were incubated overnight at 30 °C in S2-buffer (10 mM HEPES-NaOH, pH 7.2, 2 mM DTT, 50 mM NaCl, 0.5 mM EDTA, 0.015% Brij35) containing 0, 1, 2, 3, 4, and 6 M deionized urea. Residual activity was determined by adding 10 μL of sample to 500 μL of the assay mix.

Gel-Filtration Analysis. Analytical gel filtration of ODC samples (at 1−2 mg/mL) was performed using a Superose-12 10/30 column in S2-buffer at 0.2 mL/min.

Limited Proteolysis of tbODC and mODC. ODC samples (0.15−0.25 mg/mL) were incubated with trypsin or chymotrypsin at weight/weight ratios of 1/5000 to 1/200 for tbODC and 1/500 to 1/2 for mODC for 1.5 h at 37 °C in A_t buffer with 0.5 mM $CaCl_2$. The reaction was stopped by 5% TCA precipitation, and samples were analyzed by SDS−PAGE. For enzyme activity or chromatographic analysis, proteolysis was terminated by the addition of immobilized soybean trypsin inhibitor; a slurry of beads was incubated with samples for 15 min before removal by centrifugation and addition of 2 mM PMSF.

N-Terminal Sequence Determination of Proteolytic Fragments. Proteolytic fragments of tbODC and mODC were separated by SDS−PAGE. The protein was electroblotted to PDF paper as described (Matsudaira, 1987). Edman degradation was performed on an Applied Biosystems Model 470A automated sequencer using standard manufacturer's chemicals and programming.

RESULTS

Coexpression of the Putative N- and C-Terminal Domains. To test the hypothesis that the domain boundary in ODC is near amino acid 300, we attempted to coexpress the polypeptides which correspond to the two His_6-tagged putative domains, tbODC 1−305 (35.5 kDa peptide) and tbODC 306−425 (15.7 kDa peptide). Two plasmids, pT306C.N and pTΔ306C.N, were designed for expression in *E. coli* (Figure 1). In the latter plasmid the His_6-tag was deleted from the C-terminal domain sequence. To exclude any effect of translation order on the folding process, the arrangement of the tbODC fragments in the single transcription unit was residues 306−425 in the first translation unit followed by residues 1−305 in the second translation unit.

The two polypeptides are expressed in stoichiometric amounts from both plasmid constructs. The overall expression level of the coexpressed peptides and the distribution between soluble and insoluble fractions (Figure 2A,B, lanes 4 and 5) is nearly identical to that observed for wild-type tbODC (Figure 2A,B, lane 9). In both cases the soluble extracts also contained wild-type levels of ODC activity, demonstrating that the coexpressed peptides associate to form functional enzymes.

TΔ306C.N was purified to homogeneity as described previously for wild-type tbODC (Osterman et al., 1994). The kinetic characteristics (K_m = 200 μM and k_{cat} = 8 s^{-1}) of TΔ306C.N for the decarboxylation of L-ornithine are nearly identical to those obtained for wild-type tbODC (Osterman et al., 1995). TΔ306C.N also behaves identically to wild-type tbODC on Superdex 200 gel-filtration column (data not shown), displaying no visible tendency to aggregate or

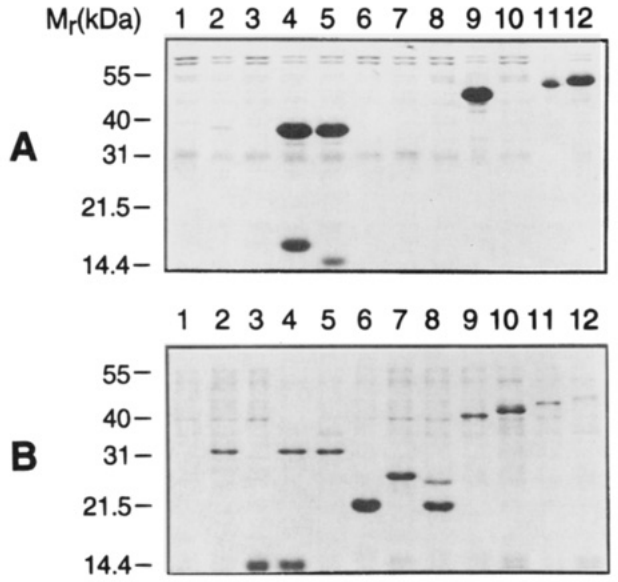

FIGURE 2: Expression of tbODC peptide fragments and chimeras. (A) Soluble *E. coli* cell extracts after partial purification on Ni^{2+}-NTA agarose minicolumns. (B) Crude pellet fractions of *E. coli* extracts dissolved in 7 M urea. Lane numbers correspond to the construct numbers in Figure 1: 1, negative control, the expression vector without a ODC insert; 2, TN305; 3, T306C; 4, T306C.N; 5, TΔ306C.N; 6, TN170; 7, T171C; 8, TΔ171C.N; 9, wild-type tbODC; 10, M170T; 11, T170M; and 12, wild-type mODC.

dissociate and forming a heterotetramer ($\alpha_2\beta_2$) identical in size to the wild-type homodimer.

Wild-type tbODC is mostly active in 1 M urea; significant denaturation (as measured by activity) did not occur until the urea concentration was greater than 1.5 M. mODC is slightly more stable in urea than tbODC (Figure 3A). This result suggests that 1 M urea might be useful as a tool to dissociate the domains without unfolding them. However, when adsorbed to the Ni^{2+}-NTA column via the His_6-tag region of the N-terminal peptide, TΔ306C.N withstands exhaustive washing by 1 M urea, 1 M NaCl or the combination without visible dissociation.

Separate Expression of the Putative N- and C-Terminal Domains. Vectors for the independent expression of the polypeptide containing amino acids 1−305 (TN305) and the polypeptide containing amino acids 306−425 (T306C) were also constructed (Figure 1). TN305 and T306C are expressed; however, most of the protein is in the pellet fraction (Figure 2, lanes 2 and 3). Expression levels of soluble TN305 and T306C in the *E. coli* cultures are at least 100-fold lower than for TΔ306C.N or wild-type tbODC (50 mg/L). Small amounts of soluble TN305 could be purified on Ni^{2+}-agarose followed by gel filtration on a Superdex G-200 column. The peptide is eluted from the latter column as a broad peak which started at the void volume and ended in the fractions corresponding to tetramers.

To test if TN305 folds into a native-like domain, mixing experiments between the purified TN305 and either wild-type tbODC or the K69A mutant were performed as previously described (Osterman et al., 1994). If TN305 forms a dimer with a full length tbODC monomer, either activation of K69A by 25% or inhibition of the wild-type enzyme by 50% would be predicted by the ideal model for a 1:1 molar mixture (Tobias & Kahana, 1993; Wente & Schachman, 1987). Because of the presence of aggregates in the purified preparation, mild denaturants (1 M urea or

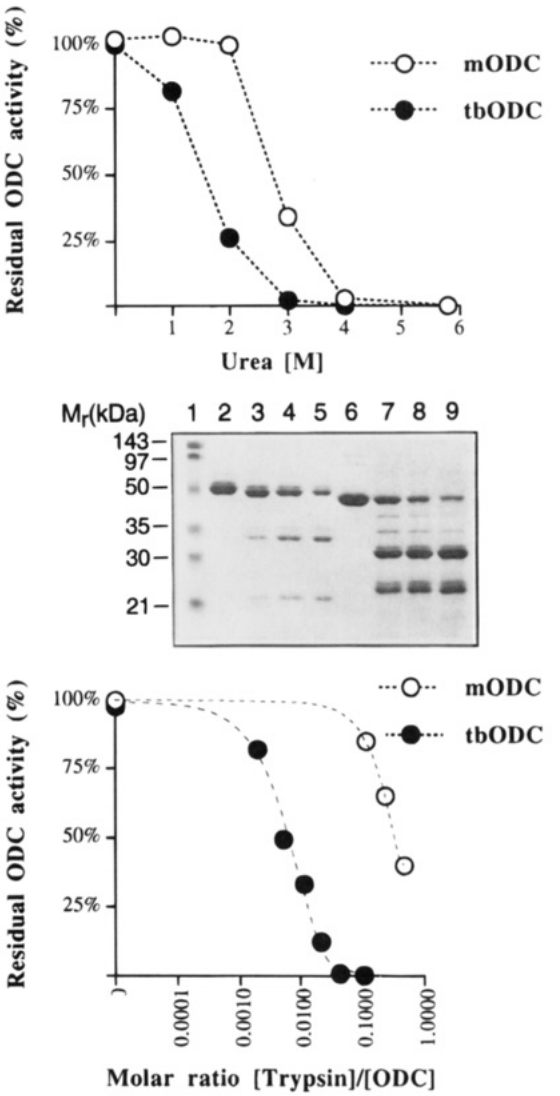

FIGURE 3: Protease and urea sensitivity of tbODC and mODC. (A, top) Urea dependence. ODC was incubated for 12 h at 30 °C in the presence of increasing concentrations of urea. Residual activity was monitored as described under Experimental Procedures. The results for mODC are similar to what was previously described (Tsirka et al., 1993). (B, middle) SDS−PAGE analysis of limited proteolysis by trypsin. Lanes 2−5, trypsin/mODC at molar ratios of 0, 1/10, 2/10, and 4/10, respectively; lanes 6−9, trypsin/tbODC at molar ratios of 0, 1/200, 2/200, and 4/200, respectively. (C, bottom) Proteolytic inactivation of mouse and *T. brucei* ODC at varying trypsin/ODC molar ratios.

0.4 M Arg) were tested. Significant inhibition of wild-type tbODC by TN305 was observed. The inhibition is time- and concentration-dependent, with the rate of inhibition accelerated by both 1 M urea and 0.4 M Arg. In 0.4 M Arg approximately a 10:1 molar ratio of TN305 to wild-type tbODC is required to achieve 50% inhibition in 3 h; 70% inhibition is observed after overnight incubation. Inhibition is also observed in the absence of Arg or urea; however, longer incubations were required. Control samples which did not contain TN305 did not lose activity during these time periods. TN305 did not complement the inactive mutant tbODC K69A, even after long incubation in the presence of more than 20-fold excess of TN305. The addition of mild denaturants (1 M urea or 0.4 M Arg) had no effect on the result.

Limited Proteolysis of T. brucei and Mouse ODC. Two major polypeptides with apparent molecular masses of 31

and 23 kDa are formed upon hydrolysis of wild-type tbODC by trypsin (Figure 3B) or chymotrypsin (data not shown). The 23-kDa trypsin fragment is further hydrolyzed to an 18-kDa fragment. On the basis of N-terminal sequence analysis of the 31 kDa fragment, the cleavage sites for trypsin and chymotrypsin hydrolysis are Arg163 and Leu161, respectively. Additional proteolysis of the 23-kDa N-terminal fragment occurs for trypsin at either Lys26 or Lys27 and for chymotrypsin within the His_6-tag region between Tyr(−5) and Phe(−4). Proteolysis of mODC by trypsin (Figure 3B) and chymotrypsin (data not shown) shows similar results except that higher protease concentrations were required (Figure 3C). The mODC C-terminal fragment (34 kDa) is likely to be larger than the tbODC (31 kDa) fragment because of the 35 amino acid C-terminal extension which is present in the primary amino acid sequence. N-terminal sequencing of the 34-kDa mODC tryptic fragment identifies two cleavage sites, Arg165 and Lys169; approximately 80% of the peptides in the isolated fragment begin with Arg165 and the remainder with Lys169. The N-terminal tryptic fragment (21 kDa) is hydrolyzed between Arg(−2) and Thr(−1) removing the His_6-tag from the N-terminus. The chymotryptic fragments of mODC were not sequenced.

The molecular weight of trypsin-cleaved tbODC is indistinguishable from wild-type tbODC by gel filtration column chromatography. The fragments can not be dissociated by 1 or 2 M urea even during gel filtration or Ni^{2+}-NTA chromatography. While the proteolytic fragments of tbODC remain tightly associated, trypsin digestion causes a parallel loss of decarboxylase activity (Figure 3B,C). ODC activity is also lost during proteolysis of mODC (Figure 3C). The activity of the fragmented tbODC is restored to 25% of wild-type levels upon mixing in a 1:1 ratio with inactive mutant tbODC C360A. Activity is not restored upon mixing of trypsin cleaved tbODC with mutant tbODC K69A.

Expression of Proteolytic Fragments and Chimeric ODCs. When expressed in *E. coli* the two proteolytic fragments of tbODC, peptide 1−170 (TN170) and 171−425 (T171C) form insoluble inclusion bodies, either when expressed independently (Figure 2A,B, lanes 6 and 7) or when coexpressed (Figure 2A,B, lane 8). Analogous constructs were also made for the expression of mODC peptides with the same result.

Chimeric proteins T170M (tbODC 1−170/mODC 171−461) and M170T (mODC 1−170/tbODC 171−425; see Figure 1) were engineered and expressed (Figure 2, lanes 10 and 11). Neither soluble protein nor ODC activity could be detected for M170T (Figure 2A,B, lane 10). In contrast, T170M is expressed as a soluble protein (Figure 2A,B, lane 11). By gel-filtration analysis T170M is eluted with retention time nearly identical to that of mODC dimer. The observed k_{cat} for decarboxylation of L-ornithine by T170M value was identical to k_{cat} for either of the two wild-type ODCs. The K_m value for the chimeric protein is 300 ± 23 μM, similar to that of wild-type tbODC (240 μM) and significantly higher than that for mODC (90 μM).

DISCUSSION

The successful reconstitution of active ODC from the coexpressed N- and C-terminal fragments (peptides 1−305 and 306−425) suggests that tbODC is composed of two domains, with a domain boundary in the region of amino acid 305. The two peptides are tightly associated into a tetramer of the same molecular weight as the native dimer and cannot be separated by denaturants prior to significant unfolding of the proteins. TΔ306C.N displays all of the typical properties of tbODC, including stoichiometric PLP-binding and kinetic characterstics (K_m and k_{cat}) for the decarboxylation of ornithine. T306C.N is also fully active, thus the His_6-tag on the 5′-end of the C-terminal domain does not affect the proper assembly of the fragmented enzyme. When alanine racemase or aspartate transcarbamoylase were reconstituted from coexpressed peptides, the complexes were 5−10 times less active than the corresponding wild-type enzymes (Toyama et al., 1991; Yang & Schachman, 1993).

When expressed separately, both the N- and C-terminal fragments are found predominately as inclusion bodies. These results suggest that the two domains may be dependent on each other to fold efficiently. Alternatively, each may fold in the absence of the other, but aggregation occurs via exposed surfaces which normally pack at the domain interface. At least for the N-terminal domain the latter explanation is supported by our ability to purify small amounts of soluble peptide, the finding that it is aggregated, and the observation that it inhibits the activity of wild-type tbODC. A 4-fold higher molar excess of TN305 is required to inhibit wild-type tbODC by 50%, when compared the double mutant tbODC K69A/C360A (Osterman et al., 1994). The requirement for higher concentrations of TN305 is likely to be caused by differential affinity between the subunits in the mixture. The purified TN305 is aggregated; thus self-association may compete with formation of the TN305/wild-type heterodimer. Additionally, because the C-terminal domain is not present, the heterodimer between TN305 and the wild-type monomer is likely to be less stable than the wild-type homodimer. The inhibition data suggest that the N-terminal domain assumes a native-like fold and that it is able to compete with the wild-type monomers to form an interaction at the dimerization interface. However, we cannot completely rule out the possibility that the inhibition of wild-type tbODC by TN305 is caused by nonspecific interactions.

Both tbODC and mODC have one major site of susceptibility to cleavage by trypsin and chymotrypsin, occurring between amino acids 160 and 170. This site is unlikely to correspond to a domain boundary because the enzyme cannot be reconstituted by coexpression of the individual peptides. The accessibility of the site suggests that it is on the protein surface contained within a loop structure. Analysis of trypsin cleavage sites in other proteins demonstrates that approximately a 12 amino acid segment lacking strong secondary structure is required for efficient cleavage (Hubbard et al., 1994). mODC is more resistant to trypsin cleavage than tbODC, suggesting that the protease site in mODC may be less likely to undergo the local unfolding required for cleavage. mODC is also more stable to inactivation by urea. In contrast, tbODC is more stable to intracellular degradation than mODC (Ghoda et al., 1990). However, as evidenced by our results, the relative *in vivo* instability of mODC is not an inherent property of the enzyme. Intracellular degradation of mODC is accelerated by interaction with the antizyme, which may act by partially denaturing the protein (Li & Coffino, 1992, 1993).

ODC inactivation upon hydrolysis by trypsin is likely to be caused by a local rather than global conformational change. Mixing of trypsin-cleaved tbODC with the inactive

mutant C360A restores activity to 25% of the wild-type levels, equivalent to what is observed when inactive N-terminal domain mutants are mixed with the C-terminal domain mutants (Osterman et al., 1995). This result is consistent with the formation of a properly folded heterodimer with one functional active site. mODC K169A is inactive (Lu et al., 1991), suggesting that trypsin hydrolysis of ODC causes loss of ODC activity by disrupting the function of Lys169.

The structure of ODC has been modeled on the basis of sequence comparison, secondary structure prediction, and hydrophobicity profiles. This analysis predicts that the N-terminal 300 amino acids of ODC fold into a β/α barrel (Grishin et al., 1995). In this model the region between residues 160 and 172 is predicted to form a surface loop (Figure 1). The findings that tbODC is organized with an N-terminal domain of 300 amino acids and that the enzyme has a protease sensitive region between residues 160 and 170 provide supporting evidence for these predictions.

Chimeric enzymes between tbODC and mODC have been successfully used to map structural differences between the two enzymes [e.g., location of the antizyme binding site (Li & Coffino, 1992, 1993)]. To extend our previous work on differential substrate binding, two chimeric enzymes were made between mODC and tbODC at the protease sensitive site. M170T forms insoluble inclusion bodies when expressed in *E. coli* and could not be kinetically characterized. T170M is expressed as a soluble active enzyme; the K_m for ornithine decarboxylation by this chimera is similar to that obtained for wild-type tbODC. A similar result was obtained for the tbODC/mODC cross-species heterodimer (Osterman et al., 1994) and in combination with the kinetic analysis of the wild-type enzyme on inhibitors suggested that a structural determinant for carboxylate binding is contributed to the active site from the same subunit as Lys69. The results from the T170M chimera suggest that this binding site can be more narrowly localized to the first 170 amino acids of the N-terminal domain.

ACKNOWLEDGMENT

We thank C. Moomaw and S. Afendis in C. Slaughter's laboratory for performing amino acid sequencing on the digested ornithine decarboxylase fragments and E. Goldsmith and N. Grishin for helpful discussions.

REFERENCES

Coleman, C. S., Stanley, B. A., & Pegg, A. E. (1993) *J. Biol. Chem. 268*, 24572−24579.
Coleman, C. S., Stanley, B. A., Viswanath, R., & Pegg, A. E. (1994) *J. Biol. Chem. 269*, 3155−3158.
Galakatos, N. G., & Walsh, C. T. (1987) *Biochemistry 26*, 8475−8480.
Ghoda, L., Phillips, M. A., Bass, K. E., Wang, C. C., & Coffino, P. (1990) *J. Biol. Chem. 265*, 11823−11826.
Grishin, N. V., Phillips, M. A., & Goldsmith, E. J. (1995) *Protein Sci. 4*, 1291−1304.
Hubbard, S. I., Eisenmenger, E., & Thornton, J. M. (1994) *Protein Sci. 3*, 757−768.
Kunkel, T. A. (1985) *Proc. Natl. Acad. Sci. U.S.A. 82*, 488.
Li, X., & Coffino, P. (1992) *Mol. Cell. Biol. 12*, 3556−3562.
Li, X., & Coffino, P. (1993) *Mol. Cell. Biol. 13*, 2377−2383.
Lu, L., Stanley, B. A., & Pegg, A. E. (1991) *Biochem J. 277*, 671−675.
Marton, L. J., & Pegg, A. E. (1995) *Annu. Rev. Pharmacol. Toxicol. 35*, 55−91.
Matsudaira, P. (1987) *J. Biol. Chem. 262*, 10035−10038.
Momany, C., Ghosh, R., & Hackert, M. L. (1995) *Protein Sci. 4*, 849−854.
Osterman, A., Grishin, N. V., Kinch, L. N., & Phillips, M. A. (1994) *Biochemistry 33*, 13662−13667.
Osterman, A., Kinch, L. N., Grishin, N. V., & Phillips, M. A. (1995) *J. Biol. Chem. 270*, 11797−11802.
Poulin, R., Lu, L., Ackerman, B., Bey, P., & Pegg, A. E. (1992) *J. Biol. Chem. 267*, 150−158.
Powers, V. M., Yang, Y. R., Fogli, M. J., & Schachman, H. K. (1993) *Protein Sci. 2*, 1001−1012.
Tabor, C. W., & Tabor, H. (1984) *Annu. Rev. Biochem. 53*, 749−790.
Tobias, K. E., & Kahana, C. (1993) *Biochemistry 32*, 5842−5847.
Toyama, H., Tanizawa, K., Yoshimura, T., Asano, S., Lim, Y. H., Esaki, N., & Soda, K. (1991) *J. Biol. Chem. 266*, 13634−13639.
Tsirka, S., & Coffino, P. (1992) *J. Biol. Chem. 267*, 23057−23062.
Tsirka, S. E., Turck, C. W., & Coffino, P. (1993) *Biochem J. 293*, 289−295.
Wang, C. C. (1995) *Annu. Rev. Pharmacol. Toxicol. 35*, 93−127.
Wente, S. R., & Schachman, H. K. (1987) *Proc. Natl. Acad. Sci. U.S.A. 84*, 31−35.
Yang, Y. R., & Schachman, H. K. (1993) *Protein Sci. 2*, 1013−1023.

BI9512760